IEEE Access
Multidisciplinary ⋮ Rapid Review ⋮ Open Access Journal

Received June 8, 2020, accepted July 6, 2020, date of publication July 16, 2020, date of current version July 29, 2020.

Digital Object Identifier 10.1109/ACCESS.2020.3009657

Downlink Transmission of Multicell Distributed Massive MIMO With Pilot Contamination Under Rician Fading

MENG WANG[1,2], DIAN-WU YUE[1], (Senior Member, IEEE), AND SI-NIAN JIN[1]
[1]College of Information Science and Technology, Dalian Maritime University, Dalian 116026, China
[2]School of Intelligence and Electronic Engineering, Dalian Neusoft University of Information, Dalian 116023, China

Corresponding author: Dian-Wu Yue (dwyue@dlmu.edu.cn)

This work was supported in part by the Natural Science Foundation of Liaoning Province under Grant 20180551028 and Grant 2019-ZD-0355, and in part by the General Project of Science and Technology Research of Liaoning Provincial Education Department under Grant JZR2019002.

ABSTRACT In this paper, we investigate the spectral efficiency (SE) of a multicell downlink (DL) distributed massive MIMO (DM-MIMO) system with pilot contamination operating over Rician fading channels in which each remote access unit (RAU) is equipped with a large number of distributed massive antenna arrays, while each user has a single antenna. In contrast to many previous works about DM-MIMO systems, the channel between users and the RAUs antennas in the same cell is modeled to be Rician fading, which is general for the 5G scenarios like Internet of Things. We explore maximum-ratio transmission (MRT) and line-of-sight (LOS) component-based equal-gain transmission (EGT) under imperfect channel state information. The tractable, but accurate closed-form expressions for the lower bounds of the achievable rate are derived for the MRT and the LOS component-based EGT over Rician fading channels in the DM-MIMO systems. Based on the obtained closed-form expressions, various power scaling laws concerning DL data transmit power and pilot transmit power are analyzed in detail. Numerical results are used to corroborate that these approximations are asymptotically tight, but accurate for systems. They also show that employing the LOS component-based EGT processing is more preferable than the MRT processing for DM-MIMO systems in conditions having a large number of RAU antennas and stronger LOS scenarios. Finally, the simulation results further show that when the number of all antennas for RAUs is fixed, the better SE performance can be obtained with more RAUs.

INDEX TERMS Distributed massive MIMO (DM-MIMO), Rician fading, line-of-sight (LOS) component, power scaling law.

I. INTRODUCTION

Massive multiple-input multiple-output (MIMO) has emerged as one of the most disruptive technologies for 5G wireless networks with the potential of enhancing system performance in terms of spectral efficiency (SE) and energy efficiency (EE) significantly [1]–[8]. By deploying hundreds of antennas at the base station (BS), uncorrelated noise, fast fading and the intra-cell interference are eliminated in the limit of infinite number of antennas [1]. Moreover, it's possible to use simple linear signal processing techniques such as maximum-ratio transmission (MRT), equal-gain transmission (EGT), zero-forcing (ZF) precoding in massive MIMO systems to achieve these advantages due to the fact that random channel vectors between BS and users tend to asymptotically orthogonal with a large number of antennas at the BS [9], [10].

On a parallel avenue, the distributed antenna systems (DAS) has gained a great deal of attention in both academic and industry because of its huge advantage in improving SE and EE, in which multiple antennas at the BS called remote antenna units (RAUs) are separately distributed in cells and assumed to be connected to a baseband processing unit (BPU) via low-delay and high-capacity backhaul links such as fibre-optic cables to shorten the average access distance between the transmitters and the users [11]–[14]. It has been shown that distributed MIMO systems are more efficient in improving achievable rate, reducing transmit

The associate editor coordinating the review of this manuscript and approving it for publication was Lei Guo.

power and enhancing cell coverage than centralized MIMO due to increased macro diversity gain and reduced average access [15]–[18].

Thanks to the promising features of massive MIMO and distributed MIMO, the combination of two concepts is an attractive candidate because of remarkable capacity gain and link reliability in addressing increasing requirements of 5G wireless networks. Some researchers have investigated the performance of distributed massive MIMO (DM-MIMO) systems widely [19]–[24]. The authors in [19] analyzed that the performance for a single-cell multi-user MIMO network with circularly distributed BS antennas and single-antenna users, and the achievable uplink (UL) rate under ZF detector was obtained analytically in closed-form. In particular, the optimal radius of the distributed antennas that maximizes the average rate of the cell was found. In [20], the SE was analytically investigated based on a novel comprehensive channel model suitable for distributed MIMO systems, where environmental and antenna physical parameters are accounted for. In [21], the problem of maximizing the EE for a downlink (DL) multicell massive DAS considering pilot contamination (PC) was formulated under a realistic power consumption model, an efficient tool by applying random matrix theory was provided to find out optimums of the number of RAUs antennas, the number of RAUs and served users to maximize the system EE. Reference [22] quantified the DL SE of multicell multi-user DM-MIMO systems with both MRT and ZF precoding in the presence of PC. The deterministic equivalence of the lower and upper bound on user ergodic achievable DL rate was derived accurately. The works in [23] focused on the beamforming training (BT) scheme in multicell multi-user distributed large-scale MIMO systems. It was revealed that the BT scheme with ZF beamforming is more preferable when the number of transmit antennas is small and/or the coherence interval is relatively large. An new algorithm is investigated in [24] by utilizing hierarchical decomposition technique and iterative successive convex approximation in a fixed single-cell network. This algorithm effectively reduced the number of activated antennas on each RAU to improve the system EE.

In previous literature of DM-MIMO systems, it is seen that the small-scale fading channels with Rayleigh distributed are assumed, so the line-of-sight (LOS) component is ignored. However in next-generation wireless communication systems, the millimeter-wave band where the impact of deterministic LOS path is dominant is expected to exploit due to a tremendous spectrum. In such condition, the Rician fading channel model where Rayleigh fading channel is regarded as a special case is more suitable for studying the system performance [25]–[30]. In [25], [26], both single-cell and multicell massive MIMO UL systems with maximum-ratio combining (MRC) and ZF were considered, authors analyzed the sum rate as well as transmit power scaling law. Under Rician fading environment, the achievable rates and the impact of the LOS component in massive MIMO amplify-and-forward full-duplex relay systems and mixed-ADC massive MIMO systems are investigated in [27], [28], respectively. The application of BT in a multicell massive MIMO system over uncorrelated Rician fading channels was presented in [29], the ranges for the length of DL pilots was found to enable that the sum SE of the scheme with BT is superior to that of the scheme without BT. The works in [30] studied performance of multicell massive MIMO systems when performing MRC detection and MRT precoding under a more practical assumption of spatially correlated Rician fading. It has been proved that the spatial correlation is of great importance and the existence of an LOS component improves the achievable SE in massive MIMO systems. In the aforementioned literature, it is seen that very few works is considered in DM-MIMO systems under the scenario of Rician fading channel.

Due to the fact that the channel state information (CSI) needs to be acquired by channel estimation which will be a heavy overhead, a linear transmission only based on the LOS component in Rician fading environment was proposed in [31]–[33], while scattered component is omitted. In particular, reference [33] studied the LOS component-based EGT (LOS-EGT) for multicell massive MIMO DL systems in Rician fading channel under imperfect CSI. It is pointed out that the LOS-EGT scheme compared to MRT can performs better when the number of BS antennas and intercell interference level are large. However, to the best of the author's knowledge, the system performance when taking into account LOS-EGT in DL multicell DM-MIMO systems has not yet been analyzed.

Different from most of the existing works, herein we consider the DL of a multicell DM-MIMO system with MRT and LOS-EGT precoding in Rician fading channel under PC where minimum mean-square error (MMSE) channel estimator is assumed. Furthermore, the achievable rate and power scaling law with respect to DL data transmit power and UL pilot transmit power are investigated. The main contributions of this paper are summarized as follows:

- The tractable but accurate closed-form lower-bound expressions which contribute to system performance analysis and establishing various power scaling properties are derived for the DL achievable rate of MRT and LOS-EGT processing under Rician fading in DM-MIMO systems, respectively. Furthermore, taking into account the environment of Rician fading enables the SE analysis of DM-MIMO systems in more practical scenarios.
- It is revealed that with MRT processing and under Rician fading in DM-MIMO systems, the DL data transmit power and the pilot transmit power of each user can be scaled down by N^{-p} and N^{-q} ($0 \leq p \leq 1$ and $q \geq 0$), respectively, while the achievable rate approaches infinity if $0 \leq p < 1$ and $q > 0$ and maintains an asymptotically unchanged user rate otherwise when the number of RAUs antennas N grows

unlimited. In addition, the effect of PC can be eliminated for the case of $q > 0$ and $N \to \infty$.

- It is shown that with LOS-EGT precoding and under Rician fading in DM-MIMO systems, the DL data transmit power of each user can be scaled down by N^{-p} ($0 \leq p \leq 1$), while the achievable rate approaches infinity if $0 \leq p < 1$ and maintains an asymptotically unchanged user rate otherwise when the number of RAUs antennas N grows unlimited. Since LOS-EGT precoding does not involve channel estimation of the fast fading component, the system performance is not affected by PC. It is also revealed that, as the number of RAUs antennas and the power of the LOS component grow without limit, all of the effects of interference from other users and uncorrelated noise disappear and the DL achievable rate will approach infinity.
- By numerical comparison with the MRT scheme, our results indicate that the LOS component-based EGT precoding scheme performs better for the case of large number of RAUs antennas and Rician K-factor. In addition, the numerical results also show that when the number of all antennas for RAUs is constant, the better SE performance can be obtained with more RAUs in multicell DM-MIMO systems which achieve a significant performance gain over the centralized massive MIMO (CM-MIMO) systems.

The remainder of this paper is organized as follows. Section II describes the DL DM-MIMO system model in Rician fading channels, MMSE channel estimation, and transmission that use MRT or LOS component-based EGT precoding. In section III, we derive the achievable rate lower bounds of these two precoding schemes and provide asymptotic analysis with the power scaling laws. Numerical results are presented in section IV, while Section V summarizes the main results of paper. Appendix gives some proofs.

Notation: We use boldface upper and lower case letters to denote matrices and column vectors, respectively. The superscripts $(\cdot)^T$ and $(\cdot)^H$ stand for transpose and conjugate-transpose, respectively. $\mathbf{I}_N$ and diag $\{a_1, \ldots, a_N\}$ stand for $N \times N$ identity matrix and diagonal matrix with diagonal elements $\{a_1, \ldots, a_N\}$, respectively. The real parts, trace, expectation, variance and covariance operators are denoted by Re$\{\cdot\}$, trace $(\cdot)$, $\mathbb{E}\{\cdot\}$, $\mathbb{V}$ar$(\cdot)$ and Cov $\{X, Y\}$ respectively. The symbol $\otimes$ denotes the Kronecker products between two matrices. Finally, we use $\mathbf{z} \sim \mathcal{CN}(\mathbf{0}, \Sigma)$ to denote a circularly symmetric complex Gaussian vector $\mathbf{z}$ with zero mean and covariance matrix Σ.

II. SYSTEM MODEL

A. SYSTEM AND CHANNEL MODEL

Consider a multicell DM-MIMO system with L hexagonal cells, where each cell consists of M RAUs equipped with N antennas for each RAU and K randomly distributed single-antenna users. We assume that $N \gg K$, which is necessary in achieving high SE in massive MIMO systems. The M RAUs in the same cell are connected to a BPU, where the main operations, including data and management processing, are implemented. We consider the system works in time-division duplex (TDD) mode so that the channel reciprocity can be exploited. An example of a seven-RAUs DM-MIMO system is shown in Fig. 1. We consider there is one RAU in the circular cell center and six RAUs evenly located on a smaller circle away from the cell center in each cell. Let $\mathbf{g}_{ilk} \in \mathbb{C}^{MN} = \left[\mathbf{g}_{i1lk}^T, \ldots, \mathbf{g}_{imlk}^T, \ldots, \mathbf{g}_{iMlk}^T\right]^T$ denote the UL channel vector from the *kth* users in the *lth* cell to all of the RAUs in the *ith* cell, where $\mathbf{g}_{imlk} \in \mathbb{C}^N$ represent the channel vector between the *mth* RAU in the *ith* cell and the *kth* user in the *lth* cell. The vector $\mathbf{g}_{ilk}$ can be expressed as

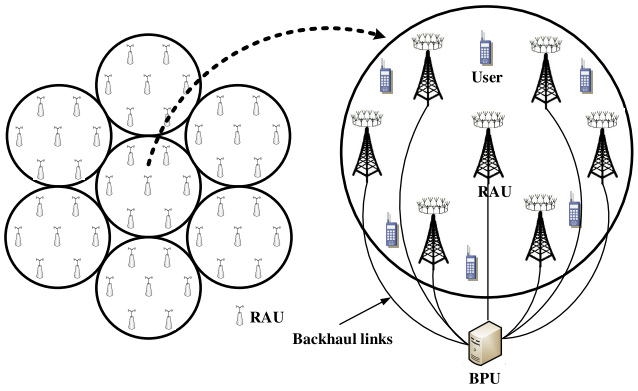

FIGURE 1. System model of multicell distributed massive MIMO.

$$\mathbf{g}_{ilk} = \mathbf{D}_{ilk}^{1/2} \mathbf{h}_{ilk} \tag{1}$$

where $\mathbf{D}_{ilk} = \text{diag}\left([\beta_{i1lk}, \ldots, \beta_{imlk}, \ldots, \beta_{iMlk}]^T\right) \otimes \mathbf{I}_N$, $\mathbf{h}_{ilk} = \left[\mathbf{h}_{i1lk}^T, \ldots, \mathbf{h}_{imlk}^T, \ldots, \mathbf{h}_{iMlk}^T\right]^T$. The β_{imlk} and $\mathbf{h}_{imlk} \in \mathbb{C}^N$ represent the large-scale fading coefficient and the fast fading channel vector between the *mth* RAU in the *ith* cell and the *kth* user in the *lth* cell, respectively. In essence, β_{imlk} models the geometric attenuation and shadow fading, which is assumed to be constant over many coherence time intervals and known *a priori* [2]. The fast fading channel vector in the different cell is a collection of Rayleigh-distributed elements. However, the fast fading channel vector between the users and the RAUs in the same cell is modeled to consist of two parts, namely a deterministic component corresponding to the LOS path and a Rayleigh-distributed random component which accounts for the scattered signals. This assumption is reasonable, since the LOS components exist in channels between the RAUs and the users in the own cell due to the short range, but, because of the scatters and buildings block, they do not exist any more in channels between the RAUs and users in different cells. As discussed in [25], [26], [33], $\mathbf{h}_{ilk}$ can be expressed as

$$\begin{cases} \left[\dfrac{\boldsymbol{\Omega}_{ik}}{\boldsymbol{\Omega}_{ik}+1}\right]^{1/2} \otimes \mathbf{I}_N \bar{\mathbf{h}}_{iik} + \left[\dfrac{1}{\Omega_{ik}+1}\right]^{1/2} \otimes \mathbf{I}_N \mathbf{h}_{w,iik}, & l = i \\ \mathbf{h}_{w,ilk}, & l \neq i \end{cases} \tag{2}$$

where $\Omega_{ik} = \text{diag}\,(K_{ik1}, \ldots, K_{ikm}, \ldots, K_{ikM})$, and $K_{ikm} \geq 0$ is the Rician K-factor of the *mth* RAU, which represents the power ratio of the LOS and fast fading components for the *kth* user in the *ith* cell. The $\mathbf{h}_{w,ilk} \in \mathbb{C}^{MN}$ is the small-scale fading channel vector, whose elements are independent and identically distributed (i.i.d.) complex random variables with zero mean and unit variance. The vector $\bar{\mathbf{h}}_{iik}$ represents the LOS component of $\mathbf{h}_{iik}$, where $\bar{\mathbf{h}}_{iik} = \left[\bar{\mathbf{h}}_{i1ik}^T, \ldots, \bar{\mathbf{h}}_{imik}^T, \ldots, \bar{\mathbf{h}}_{iMik}^T\right]^T$. The vector $\bar{\mathbf{h}}_{imik}$ is governed by steering response of uniform linear array (ULA) with a LOS direction of departure and can be expressed as [33], [34]

$$\left[1, \ldots, e^{-j(n-1)\frac{2\pi d}{\lambda}\sin(\theta_{ikm})}, \ldots, e^{-j(N-1)\frac{2\pi d}{\lambda}\sin(\theta_{ikm})}\right]^T \quad (3)$$

where λ is the carrier wavelength, θ_{ikm} is the departure angle of the *kth* user in the *ith* cell for *mth* RAU and d is the antenna spacing. In general, the physical size of the antenna array can be very small at high frequencies, so we set $d = \lambda/2$ and $\theta_{ikm} \in [-\pi, \pi]$ [34].

B. CHANNEL ESTIMATION

We assume that the multicell system is a TDD system with channel reciprocity property. In practice, $\mathbf{g}_{ilk}$ is usually estimated by utilizing pilot sequences at the BS. Since the LOS component changes slowly, the BS can estimate the LOS component very accurately with negligible signaling overhead. As in [25], $\bar{\mathbf{h}}_{iik}$ and Ω_{ik} are assumed to be known at both the RAUs and the users. Therefore, the channel estimation $\hat{\mathbf{g}}_{w,ilk}$ is given by [25]

$$\begin{cases} \left[\dfrac{\boldsymbol{\Omega}_{ik}}{\boldsymbol{\Omega}_{ik}+1}\right]^{1/2} \otimes \mathbf{I}_N \bar{\mathbf{g}}_{iik} + \left[\dfrac{1}{\Omega_{ik}+1}\right]^{1/2} \otimes \mathbf{I}_N \hat{\mathbf{g}}_{w,iik}, & l = i \\ \hat{\mathbf{g}}_{w,ilk}, & l \neq i \end{cases} \quad (4)$$

where $\bar{\mathbf{g}}_{iik} = \mathbf{D}_{iik}^{1/2}\bar{\mathbf{h}}_{iik}$ and $\hat{\mathbf{g}}_{w,ilk}$ represents the estimate of the random vector $\mathbf{g}_{w,ilk} = \mathbf{D}_{ilk}^{1/2}\mathbf{h}_{w,ilk}$. During UL pilot transmission phase, all the user simultaneously transmit pilot sequences with length τ_u and power p_u. we assume that the pilot sequences of users in the same cell are pairwisely orthogonal, and the same set of pilot sequences is reused in every different cell. In this case, the channel estimate from the UL pilots is contaminated by the users from other cells using the same pilot. Considering pilot contamination, the MMSE estimate of $\mathbf{g}_{w,ilk}$ can be written as [25], [35]

$$\hat{\mathbf{g}}_{w,ilk} = \mathbf{D}_{ilk}\mathbf{Q}_{ik}^{-1}\left(\sum_{l=1}^{L}\mathbf{g}_{w,ilk} + \frac{1}{\sqrt{\tau_u p_u}}\mathbf{z}_{ik}\right) \quad (5)$$

where $\mathbf{Q}_{ik} = \sum_{l=1}^{L}\mathbf{D}_{ilk} + \frac{1}{\tau_u p_u}\mathbf{I}_{MN}$, the entries of $\mathbf{z}_{ik} \in \mathbb{C}^{MN}$ are i.i.d. $\mathcal{CN}(0,1)$ random variables and we define $\hat{\mathbf{h}}_{i,k} \triangleq \mathbf{Q}_{ik}^{-1/2}\left(\sum_{l=1}^{L}\mathbf{g}_{w,ilk} + \frac{1}{\sqrt{\tau_u p_u}}\mathbf{z}_{ik}\right)$ which can be shown to be distributed as $\hat{\mathbf{h}}_{i,k} = \left[\hat{\mathbf{h}}_{ik1}^T, \ldots, \hat{\mathbf{h}}_{ikm}^T, \ldots, \hat{\mathbf{h}}_{ikM}^T\right]^T \sim \mathcal{CN}(\mathbf{0}, \mathbf{I}_{MN})$. We can rewritten $\hat{\mathbf{g}}_{w,ilk}$ as

$$\hat{\mathbf{g}}_{w,ilk} = \text{diag}\left([\lambda_{i1lk}, \ldots, \lambda_{imlk}, \ldots, \lambda_{iMlk}]^T\right) \otimes \mathbf{I}_N \times \left[\hat{\mathbf{h}}_{ik1}^T, \ldots, \hat{\mathbf{h}}_{ikm}^T, \ldots, \hat{\mathbf{h}}_{ikM}^T\right]^T \quad (6)$$

where $\lambda_{imlk} = \beta_{imlk}\left(\sum_{l=1}^{L}\beta_{imlk} + \frac{1}{\tau_u p_u}\right)^{-1/2}$. λ_{imlk} represents the equivalent large scale fading which is assumed that the realizations are perfectly known to the RAUs as in [1], and $\hat{\mathbf{h}}_{ikM}^T$ represents the equivalent Rayleigh fading part of the estimated channel. The equivalent channel model in (6) will be used to simplify the theoretical analysis. We can decompose the $\mathbf{g}_{w,ilk}$ as $\mathbf{g}_{w,ilk} = \hat{\mathbf{g}}_{w,ilk} + \tilde{\mathbf{g}}_{w,ilk}$, where $\tilde{\mathbf{g}}_{w,ilk} \sim \mathcal{CN}\left(\mathbf{0}, \mathbf{D}_{ilk} - \mathbf{D}_{ilk}^2\mathbf{Q}_{ik}^{-1}\right)$ is the estimation error vector which is statistically independent of $\hat{\mathbf{g}}_{w,ilk}$ under the MMSE estimation. It also can be shown that the estimated channel vector $\hat{\mathbf{g}}_{w,ilk}$ and $\hat{\mathbf{g}}_{w,iik}$ become correlated random vectors with correlation matrix $\text{Cov}\left(\hat{\mathbf{g}}_{w,iik}, \hat{\mathbf{g}}_{w,ilk}\right) = \mathbf{D}_{iik}\mathbf{Q}_{lk}^{-1}\mathbf{D}_{ilk}$ due to the effect of PC.

C. DOWNLINK TRANSMISSION

For DL data transmission, we assume that all the M RAUs in each cell transmit data to K users. The DL received signal at the *kth* user in the *ith* cell is given by

$$r_{ik} = \sqrt{p_d}\sum_{l=1}^{L}\sum_{m=1}^{M}\mathbf{g}_{lmik}^T\mathbf{W}_{lm}\mathbf{s}_{lm} + n_{ik} \quad (7)$$

where p_d is the transmit power, $n_{ik} \sim \mathcal{CN}(0,1)$ is the noise term at the *kth* user in the *ith* cell, and $\mathbf{s}_{lm} \in \mathbb{C}^K = [s_{lm1}, \cdots, s_{lmK}]^T$ is the transmit signal vector of *mth* RAU for users in the *lth* cell with $\mathbb{E}\{\mathbf{s}_{lm}\} = \mathbf{0}$ and $\mathbb{E}\left\{\mathbf{s}_{lm}\mathbf{s}_{lm}^H\right\} = \mathbf{I}_K$. The $\mathbf{W}_{lm} = \alpha_l\mathbf{A}_{lm}^*$ is the precoding matrix of the *mth* RAU in the *lth* cell, and α_l normalizes the transmit power in the *lth* cell so that $\mathbb{E}\left\{\sum_{m=1}^{M} tr\left(\mathbf{W}_{lm}\mathbf{W}_{lm}^H\right)\right\} = 1$.

As mentioned before, MRT precoding is simple linear signal processing method and relatively easy to implement and analyze. On the other hand, EGT precoding can be implemented with low-complexity hardware. In particular, the LOS-EGT scheme is only based on the LOS component [33], [36]. Hence the channel estimation of the scattered component is ignored, and overhead for acquiring CSI will be significantly reduced. Therefore we are also interested in LOS-EGT scheme. When the RAUs perform MRT precoding, $\mathbf{a}_{lmk}^{MRT} = \hat{\mathbf{g}}_{lmlk}$ and α_l can be obtained as

$$\alpha_l = \frac{1}{\sqrt{N\sum_{k=1}^{K}\sum_{m=1}^{M}\left(\frac{K_{lkm}\beta_{lmlk}+\lambda_{lmlk}^2}{K_{lkm}+1}\right)}} \quad (8)$$

where $\mathbf{a}_{lmk}$ denotes the *kth* column vector of $\mathbf{A}_{lm}$. For LOS component-based EGT processing, the $\alpha_l = 1/\sqrt{MNK}$ and $\mathbf{a}_{lmk}^{LOS-EGT} = \bar{\mathbf{h}}_{lmlk}$, respectively. We adopt the same assumption as in [3], [37] that the channel estimation is available at the RAUs, and each user detects its desired

signal based only on the statistical properties of the channel $\mathbb{E}\left\{\mathbf{a}_{imk}^H \mathbf{g}_{imik}\right\}$. Therefore, the expression in (7) can be rewritten and expanded as

$$\begin{aligned} r_{ik} &= \alpha_i \sqrt{p_d} \sum_{m=1}^{M} \mathbb{E}\left\{\mathbf{a}_{imk}^H \mathbf{g}_{imik}\right\} s_{imk} \\ &+ \alpha_i \sqrt{p_d} \sum_{m=1}^{M} \left(\mathbf{a}_{imk}^H \mathbf{g}_{imik} - \mathbb{E}\left\{\mathbf{a}_{imk}^H \mathbf{g}_{imik}\right\}\right) s_{imk} \\ &+ \alpha_i \sqrt{p_d} \sum_{j=1, j\neq k}^{K} \sum_{m=1}^{M} \mathbf{a}_{imj}^H \mathbf{g}_{imik} s_{imj} \\ &+ \sum_{l=1, l\neq i}^{L} \sum_{j=1}^{K} \sum_{m=1}^{M} \alpha_i \sqrt{p_d} \mathbf{a}_{lmj}^H \mathbf{g}_{lmik} s_{lmj} + n_{ik} \end{aligned} \tag{9}$$

where the first term is the desired signal, and other terms can be treated as the effective noises. From (9), the lower bound on achievable rate of the *kth* user in the *ith* cell can be given by

$$R_{ik} = \log_2\left(1 + \mathrm{SINR}_{ik}\right) \tag{10}$$

where the signal-to-interference-plus-noise ratio (SINR) can given by (11), as shown at the bottom of the page.

III. DOWNLINK RATE ANALYSIS

A. MRT UNDER RICIAN FADING

Theorem 1: When MRT precoding is employed in Rician fading, the lower bound on the desired user's achievable rate in (10) is given in closed form as (12), as shown at the bottom of the next page. where

$$\Delta_1 = \left[\alpha_i N \sum_{m=1}^{M} \left(\frac{\lambda_{imik}^2 + \beta_{imik} K_{ikm}}{K_{ikm} + 1}\right)\right]^2 \tag{13}$$

$$\Delta_2 = \alpha_l^2 N \sum_{m=1}^{M} \frac{\beta_{lmik}\left(\lambda_{lmlj}^2 + \beta_{lmlj} K_{ljm}\right)}{\left(K_{ljm} + 1\right)} \tag{14}$$

$$\begin{aligned} \Delta_3 &= \alpha_l^2 N \sum_{m=1}^{M} \frac{\beta_{lmik}\left(\lambda_{lmlk}^2 + \beta_{lmlk} K_{lkm}\right)}{\left(K_{lkm} + 1\right)} \\ &+ \left[\alpha_l N \sum_{m=1}^{M} \left(\frac{1}{K_{lkm} + 1}\right)^{1/2} \lambda_{lmlk} \lambda_{lmik}\right]^2 \end{aligned} \tag{15}$$

$$\begin{aligned} \Delta_4 &= \alpha_i^2 N \sum_{m=1}^{M} \frac{\beta_{imik}\left(\lambda_{imij}^2 + \lambda_{imij}^2 K_{ikm} + \beta_{imij} K_{ijm}\right)}{\left(K_{ijm} + 1\right)\left(K_{ikm} + 1\right)} \\ &+ \left[\sum_{m=1}^{M} \alpha_i \Delta_{ikjm} \sqrt{\frac{\beta_{imik}\beta_{imij} K_{ikm} K_{ijm}}{\left(K_{ikm} + 1\right)\left(K_{ijm} + 1\right)}}\right]^2 \end{aligned} \tag{16}$$

$$\Delta_{ikjm} = \frac{\sin\left(\frac{N\pi}{2}\left[\sin\left(\theta_{ikm}\right) - \sin\left(\theta_{ijm}\right)\right]\right)}{\sin\left(\frac{\pi}{2}\left[\sin\left(\theta_{ikm}\right) - \sin\left(\theta_{ijm}\right)\right]\right)} \tag{17}$$

Proof: Please refer to Appendix B.

We investigate the potential of power saving in the data transmission phase of the system when the RAUs are equipped with a massive antenna array. Without loss of generality, we let p_d and p_u scale down proportionally by the factor of $E_d/N^p (p \geq 0)$ and $E_u/N^q (q \geq 0)$, respectively, i.e $p_d = E_d/N^p$ and $p_u = E_u/N^q$, where transmit power E_d and pilot power E_u are fixed regardless of N. In addition, we let $\alpha_l' = \alpha_l\sqrt{N}$ such that α_l' is a constant. As $N \to \infty$, the power scaling laws for the considered system are provided in the following cases.

1) *Case 1:* Assume that the pilot power p_u is a constant and save the transmit power p_d, i.e. $q = 0$, which corresponds to the case where channel estimation accuracy remains unchanged. The *Corollary 1* and *Corollary 2* in the following that any choice of $0 \leq p \leq 1$ is able to maintain system's target rate are provided.

Corollary 1: With $p_d = E_d/N^p$ and E_d fixed, where $0 \leq p < 1$, the lower bound on the achievable rate limit of DM-MIMO system is given by (18), as shown at the bottom of the next page.

Corollary 2: With $p_d = E_d/N^p$ and E_d fixed, where $p = 1$, the lower bound on the achievable rate limit of DM-MIMO system is given by (19), as shown at the bottom of the next page.

It can be seen from *Corollary 1* and *Corollary 2* that, as $N \to \infty$, the effect of channel estimation error, the intra-cell and inter-cell transmission interference from the users that use different pilot sequences is eliminated completely. In particular, the impact of uncorrelated received noise also vanishes, and the correlated interference from other cells due to the reuse of the same pilot sequences becomes the only remaining factor for MRT precoding in *Corollary 1*. It also implies that the transmit power of each user can be scaled down to E_d/N^p $(0 \leq p \leq 1)$, and p_u is a constant while maintaining the same performance for increasing N. we can also observe that for an unlimited value of N, in spite of p_d and p_u not being scaled down, i.e. $p = q = 0$, the ultimate rate converges to a constant which is only related to PC. From *Corollary 2*, it is not difficult to observe that the DL sum rate improves as the transmit power p_d increases. However, the DL sum rate becomes saturation in the high signal-to-noise ratio (SNR) regime due to the interference-limited at high SNR for the system in signal transmission phase. *Corollary 1* and *Corollary 2* also reveal that using the higher pilot power p_u does not yield the better DL sum rate performance due to increased pilot

$$\mathrm{SINR}_{ik} = \frac{p_d \left|\mathbb{E}\left\{\alpha_i \mathbf{g}_{iik}^H \hat{\mathbf{g}}_{iik}\right\}\right|^2}{p_d \sum_{(l,j)\neq(i,k)} \mathbb{E}\left\{\left|\alpha_l \mathbf{g}_{lik}^H \hat{\mathbf{g}}_{llj}\right|^2\right\} + p_d \mathbb{V}\mathrm{ar}\left\{\alpha_i \mathbf{g}_{iik}^H \hat{\mathbf{g}}_{iik}\right\} + 1} \tag{11}$$

interference from other cells at the same time. In addition, it is worth pointing that the power scaling laws with imperfect CSI depend on the value of the Rician K-factor. For a very strong LOS scenario, i.e., $K_{ikm} \to \infty$, $(i = 1, \cdots, L; k = 1, \cdots, N; m = 1, \cdots, M)$, where the channel estimation becomes far more robust. The (19) converges to

$$R^{MRT}_{ik,\,\text{Rician}} \to \log_2\left[1 + E_d\left(\alpha_i' \sum_{m=1}^{M} \beta_{imik}\right)^2\right] \tag{20}$$

2) *Case 2:* We also consider the potential for saving pilot power p_u, i.e. $q > 0$, which corresponds to the case where channel estimation accuracy is decreased. The different achievable rates are provided in the following *Corollary 3* and *Corollary 4* when $0 \le p \le 1$.

Corollary 3: With $p_d = E_d/N^p$, $p_u = E_u/N^q$ and E_d, E_u fixed, where $p = 1$, $K_{ikm} > 0$, the lower bound on the achievable rate limit of DM-MIMO system is given by

$$R^{MRT}_{ik,\,\text{Rician}} \to \log_2\left(1 + E_d\left[\alpha_i' \sum_{m=1}^{M}\left(\frac{\beta_{imik}K_{ikm}}{K_{ikm}+1}\right)\right]^2\right) \tag{21}$$

Corollary 4: With $p_d = E_d/N^p$, $p_u = E_u/N^q$ and E_d, E_u fixed, where $0 \le p < 1$, the lower bound on the achievable rate limit of DM-MIMO system tends to infinity, i.e., $R^{MRT}_{ik,Rician} \to \infty$.

Corollary 3 and *Corollary 4* reveal that for any $q > 0$, all the effect of transmission interference and channel estimation error can be eliminated, which indicates that the effect of PC vanishes. We can eliminate the effect of PC by scaling down the UL pilot transmit power as the number of RAUs antennas grows unlimited in multicell DM-MIMO systems over Rician fading channels with MRT processing. Furthermore, the Rician K-factor and large scale fading coefficient become the only two factors that influence the system performance in *Corollary 3*, and the achievable rate of system tends to infinity even though the transmit power is scaled down in *Corollary 4*. It also indicates that the large-scale antenna array is beneficial to improving the performance of systems. For a very strong LOS scenario, i.e., $K_{ikm} \to \infty$, $(i = 1, \cdots, L; k = 1, \cdots, N; m = 1, \cdots, M)$, the (21) also converges to (20).

B. LOS-EGT UNDER RICIAN FADING

Theorem 2: When the LOS component-based EGT precoding is employed in Rician fading, the lower bound on the desired user's achievable rate in (10) is given in closed form as (22), as shown at the bottom of the page.

Proof: Please refer to Appendix C.

Due to the fact that the channel estimation of the scattered component is negligible, we only need to try to find the potential for saving transmit power p_d. Based on (22), *Corollary 5* and *Corollary 6* state power scaling laws of LOS-EGT precoding under Rician fading.

Corollary 5: With $p_d = E_d/N^p$, and E_d fixed, where $0 \le p < 1$, when N grows unboundedly, lower bound on the achievable rate limit of DM-MIMO system tends to infinity, i.e., $R^{LOS-EGT}_{ik,Rician} \to \infty$.

$$R_{ik} = \log_2\left(1 + \frac{\Delta_1}{\sum_{l=1,l\neq i}\sum_{j=1,j\neq k}^{L}\Delta_2 + \sum_{l=1,l\neq i}^{L}\Delta_3 + \sum_{j=1}^{K}\Delta_4 + \frac{1}{p_d}}\right) \tag{12}$$

$$R^{MRT}_{ik,\text{Rician}} \to \log_2\left(1 + \frac{\left[\alpha_i'\sum_{m=1}^{M}\left(\frac{\lambda^2_{imik}+\beta_{imik}K_{ikm}}{K_{ikm}+1}\right)\right]^2}{\sum_{l=1,1\neq i}^{L}\left[\alpha_l'\sum_{m=1}^{M}\left(\frac{1}{K_{lkm}+1}\right)^{1/2}\lambda_{lmlk}\lambda_{lmik}\right]^2}\right) \tag{18}$$

$$R^{MRT}_{ik,\,\text{Rician}} \to \log_2\left(1 + \frac{E_d\left[\alpha_i'\sum_{m=1}^{M}\left(\frac{\lambda^2_{imik}+\beta_{imik}K_{ikm}}{K_{ikm}+1}\right)\right]^2}{E_d\sum_{l=1,1\neq i}^{L}\left[\alpha_l'\sum_{m=1}^{M}\left(\frac{1}{K_{lkm}+1}\right)^{1/2}\lambda_{lmlk}\lambda_{lmik}\right]^2 + 1}\right) \tag{19}$$

$$R^{LOS-EGT}_{ik,\text{Rician}} \to \log_2\left(1 + \frac{\left[\sum_{m=1}^{M}\left(\frac{K_{ikm}\beta_{imik}}{K_{ikm}+1}\right)^{1/2}\right]^2}{\frac{K}{N}\sum_{m=1}^{M}\left(\frac{\beta_{imik}}{K_{ikm}+1}\right) + \frac{1}{N^2}\sum_{j=1,j\neq k}^{K}\sum_{m=1}^{M}\left(\Delta^2_{ikjm}\frac{\beta_{imik}K_{ikm}}{K_{ikm}+1}\right) + \frac{K}{N}\sum_{l=1,l\neq i}^{L}\sum_{m=1}^{M}\beta_{lmik} + \frac{MK}{p_dN}}\right) \tag{22}$$

Corollary 6: With $p_d = E_d/N^p$, and E_d fixed, where $p = 1$, when N grows unboundedly and $K_{ikm} > 0$, lower bound on the achievable rate limit of DM-MIMO system converges to a constant as

$$R_{ik,\,\text{Rician}}^{\text{LOS-EGT}} \to \log_2\left(1 + \frac{E_d}{MK}\left[\sum_{m=1}^{M}\left(\frac{\beta_{imik}K_{ikm}}{K_{ikm}+1}\right)^{\frac{1}{2}}\right]^2\right) \tag{23}$$

Corollary 5 shows that all the transmission interference from the users and the impact of uncorrelated received noise are negligible with LOS-EGT precoding when $N \to \infty$, and the achievable rate of system tends to infinity. Since the channel estimation of the scattered component is not involved for the LOS-EGT processing, we only use the information of the LOS component as a channel estimation without the need for sending UL pilot power. It reveals that the LOS-EGT precoding is not impacted by PC, this is the reason why the DL rate performance are the same in *Corollary 4* and *Corollary 5*. Comparing *Corollary 2*, *Corollary 3* and *Corollary 6*, we also find that the transmit power can be scaled down by N^{-1} while guaranteeing an asymptotically unchanged rate for Rician fading. For a very strong LOS scenario, i.e., $K_{ikm} \to \infty$, $(i = 1, \cdots, L; k = 1, \cdots, N; m = 1, \cdots, M)$, the (23) converges to

$$R_{ik,\,\text{Rician}}^{\text{LOS}-\text{EGT}} \to \log_2\left[1 + \frac{E_d}{MK}\left(\sum_{m=1}^{M}\sqrt{\beta_{imik}}\right)^2\right] \tag{24}$$

Corollary 7: When $K_{ikm} \to \infty$, $(i = 1, \cdots, L; k = 1, \cdots, N; m = 1, \cdots, M)$, the lower bound on the achievable rate limit of DM-MIMO system tends to (25), as shown at the bottom of the next page.

This conclusion indicates that when the Rician K-factor grows unboundedly, the lower bound on the DL achievable rate will converge to a fixed value. If N grows without limit, then the achievable rate in (22) will tend to infinity. It reveals that the effects of all the transmission interference and uncorrelated received noise disappear when the number of RAUs antennas and Rician K-factor go to infinity.

Before finishing this section, it is pointed that the power scaling laws for MRT and LOS-EGT precoding studied in Section III are all under the case of not considering the jamming attacks. However, robustness against jamming attacks have been recognized as an important requirement that future networks must fulfill in massive MIMO systems [38]–[40]. The authors in [38] and [39] examined the secrecy performance and optimal power allocation of a two-way relaying network in the existence of a friendly jammer and an adversary jammer respectively. Research on the framework for protecting the UL transmission of a massive MIMO system from a jamming attack have been proposed and attracted strong interests recently [40]. But the issues of jamming attack in the pilot phase on the DM-MIMO system performance are beyond the scope of this paper and left for our further works.

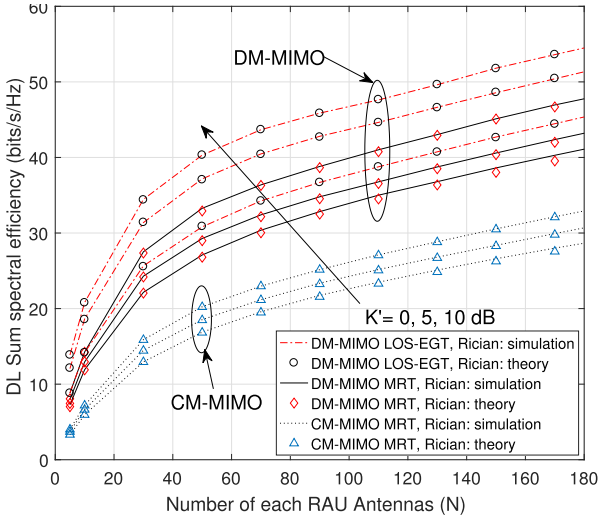

FIGURE 2. Effect of the number of each RAU antennas on the DL sum spectral efficiency of DM-MIMO system and CM-MIMO system.

IV. NUMERICAL RESULT AND DISCUSSIONS

In this section, the analytical results in the previous section are validated and evaluated by numerical simulations. In the simulation, we define a seven-cell setup and a frequency reuse factor of 1. We consider the seven-RAU DM-MIMO system as shown in Fig. 1. There are K=10 users that are located uniformly at random in each cell. The radius of each cell is set to be $R_c = 2000$ meters. The length of UL transmit pilot sequences is $\tau_u = K$ and there are $T = 196$ symbols in each frame [2]. The large scale fading factor is generated as $\beta_{imlk} = 1/d_{imlk}^{\tau}$, where d_{imlk} is the distance between the *mth* RAU in the *ith* cell and the *kth* user in the *lth* cell, and $\tau = 2.5$ is the path-loss exponent. For DM-MIMO system, the large scale fading factor between the *kth* user and the RAUs with minimum distance to the *kth* user in the *ith* cell is scaled with $M^{\tau/2}$, while the average distances between the *kth* user and other $M-1$ RAUs in the *ith* cell and the average distances between the *kth* user in the *ith* cell and the RAUs in other cells can be only determined by the cell radius R_c, so all of the large scale fading factors are chosen as given in [21]. For convenience, we assume users with Rician fading have the same Rician K-factor, denoted by K'.

For the comparison of the sum rates obtained with MRT and LOS-EGT precoding, we consider the DL sum SE (sum rate in bits/s/Hz) in *ith* cell which is defined as

$$C_i = \lambda_p \sum_{k=1}^{K} R_{ik} \tag{26}$$

where λ_p is the pilot overhead associated with the DL rate expressions. In particular, $\lambda_p = \frac{T-\tau_u}{T}$ for MRT processing, whereas $\lambda_p = 1$ for LOS-EGT processing.

In Fig. 2, we compare the DL sum spectral efficiencies per cell of MRT and LOS-EGT precoding under Rician fading in DM-MIMO systems, and MRT precoding under Rician fading in CM-MIMO systems for $p_u = p_d = 10$dB.

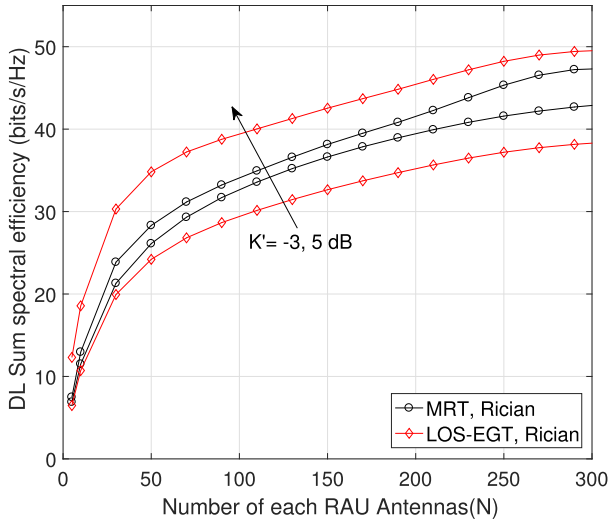

FIGURE 3. Effect of the number of each RAU antennas on the DL sum spectral efficiency under power scaling laws.

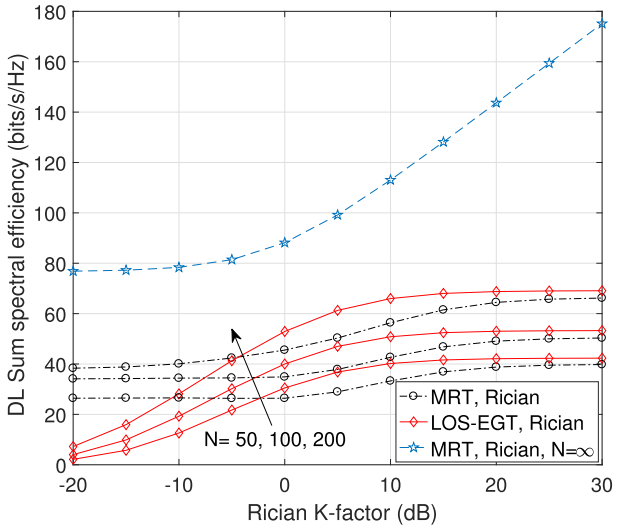

FIGURE 4. Effect of the Rician K-factor on the DL sum spectral efficiency.

Results are shown for three different Rician K-factor, which are $K' = 0$dB, $K' = 5$dB and $K' = 10$dB, respectively. Clearly, it can be observed that our derived analytical results match well with simulation results in all cases. The DL sum rates significantly increase with increasing K'. As seen from the figure, since the large path losses of the transmit signals are avoided by introducing the RAUs, the achievable rate of the DM-MIMO system is much larger than that of the CM-MIMO system. It also shows that the rate performance of LOS-EGT precoding is better than that of MRT precoding with Rician fading channel in DM-MIMO system because of the fact that the LOS-EGT precoding requires the least amount of pilot overhead and is free from PC. Due to the tightness between the simulation and the approximation results, we will use the closed-form expressions for next numerical simulation.

In Fig. 3, we validate the power scaling laws established for MRT and LOS-EGT precoding with different Rician K-factors, which are $K' = -3$dB and $K' = 5$dB. In simulation, we set $p_d = E_d/N$, $p_u = E_u/N$ and $E_u = E_d = 20$dB for examining the power scaling laws of MRT precoding and set $p_d = E_d/N$ for examining the power scaling laws of LOS-EGT. As excepted, when $K' = -3$dB, the DL sum rates gradually increase and converge to constant values when the number of each RAU antennas grows unlimited with MRT and LOS-EGT precoding. There is a balance between the increase and decrease of the DL sum rate brought by the increased N and scaled down the power. Therefore, the DL sum rate performance is shown to saturate with a increased N. It can also be seen that the rate performance of LOS-EGT precoding is better than that of MRT. All observations conform to our analysis.

In Fig. 4 shows how the sum spectral efficiencies vary with Rician K-factor when $N = 50$, $N = 100$, $N = 200$ and $p_u = p_d = 10$dB. Clearly, the DL sum rates grow as the Rician K-factor increases and tend to fixed values for the MRT and LOS-EGT precoding schemes. It reveals that the addition of Rician K-factor can improve the DL performance. It can be also observed that the effect of large N is significant. The DL sum rate grows infinitely for increasing Rician K-factor with unlimited N for MRT precoding. In this figure, it is also shown that for sufficiently large Rician K-factor, LOS-EGT precoding has a better rate performance due to saving pilot overhead. We notice that all the interference and noise are negligible for very large Rician K-factor and N.

Fig. 5 plots the DL sum spectral efficiencies versus the SNR for MRT and LOS-EGT precoding, respectively. For this figure, we set $N = 50$, $N = 200$, and $K' = 5$dB. The system of MRT shows performance advantage over the system of LOS-EGT when SNR is small. However, as the DL SNR increases gradually, the DL sum rate performance of LOS-EGT precoding is better than that of MRT precoding because of being free from PC. We also notice that the DL sum rate performance is shown to saturate in the large SNR regime due to the effect of interference. Therefore, it can be concluded that the scheme of LOS-EGT precoding has the better performance advantage in multicell DM-MIMO systems over Rician fading channels.

$$R_{ik,\,\text{Rician}}^{\text{LOS-EGT}} \to \log_2\left(1+\frac{N\left(\sum_{m=1}^{M}\sqrt{\beta_{imik}}\right)^2}{\frac{1}{N}\sum_{j=1,j\neq k}^{K}\sum_{m=1}^{M}\left(\Delta_{ikjm}^2\beta_{imik}\right)+K\sum_{l=1,l\neq i}^{L}\sum_{m=1}^{M}\beta_{lmik}+\frac{MK}{p_d}}\right) \tag{25}$$

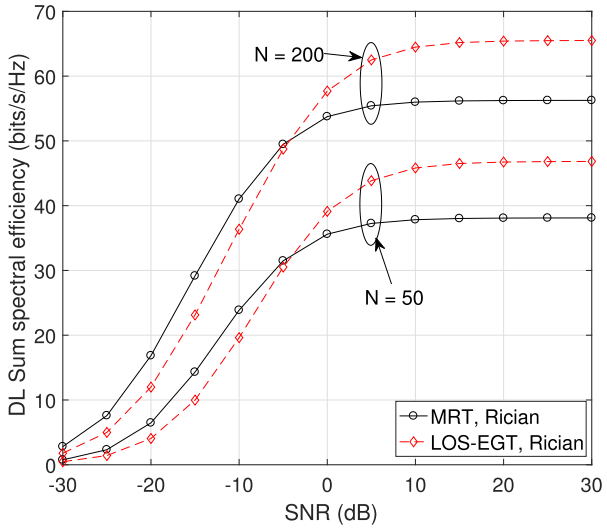

FIGURE 5. Effect of SNR on the DL sum spectral efficiency.

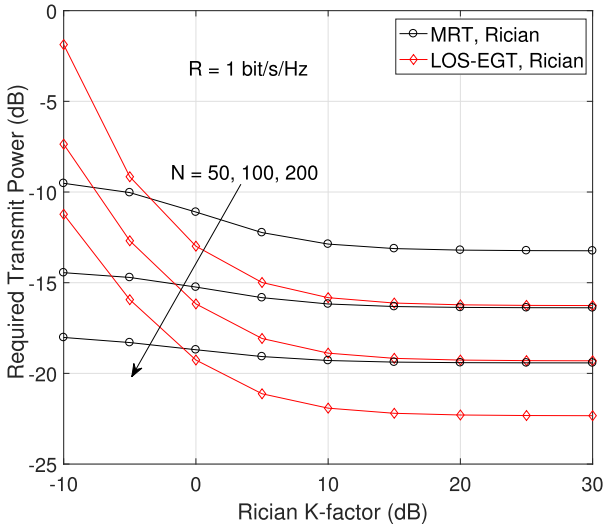

FIGURE 6. Effect of the Rician K-factor on the required transmit power to achieve 1bit/s/Hz each user.

Fig. 6 illustrates the effect of the Rician K-factor to reduce the transmit power under a fixed DL sum rate and the settings of $N = 50$, $N = 100$, $N = 200$ and $p_u = p_d = 10$dB. From Fig. 6, the observations show that to maintain the same DL sum rate, the transmit power can be cut down as the increase of the Rician K-factor, which implies the improvement effect of the Rician K-factor on the DL sum spectral efficiencies performance. It is also found that the required transmit power decreases with the growth of the number of each RAU antennas N, which reveals that the increased N can also improve the DL sum rate. We can also see that the required transmit power for the system of LOS-EGT precoding can be cut down more than that of MRT precoding when Rician K-factor is large in order to maintain the same DL sum rate performance, and vice verse. Therefore, it can be concluded that LOS-EGT precoding for a larger Rician K-factor could

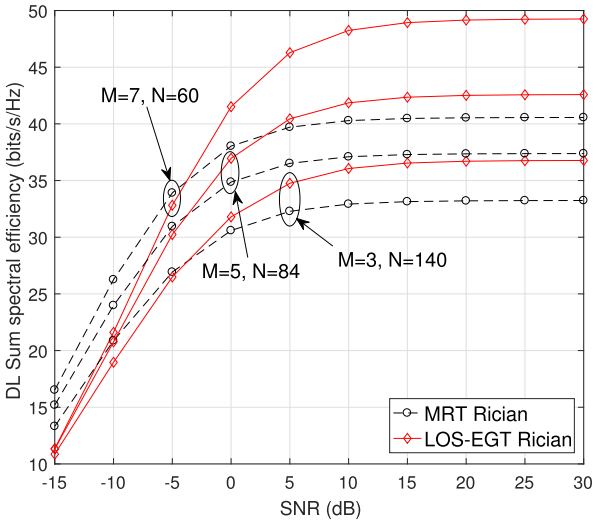

FIGURE 7. Effect of SNR on the DL sum spectral efficiency when $M = 3$, $N = 140$; $M = 5$, $N = 84$ and $M = 7$, $N = 60$.

provide a better performance under multicell DM-MIMO systems over Rician channels.

Fig. 7 describes the DL sum spectral efficiencies versus the SNR for MRT and LOS-EGT precoding and compares the DL sum spectral efficiencies for different cases with various numbers of RAUs and antennas for each RAU, where $M = 3$, $N = 140$; $M = 5$, $N = 84$ and $M = 7$, $N = 60$ under a fixed number of all antennas for RAUs in multicell DM-MIMO system are considered, respectively. As can be seen from fig. 7, when $M = 7$, $N = 60$, the system provides the best DL sum rate performance which is because that average access distance becomes shorter when the number of RAUs increases. We notice that, with more RAUs, the better SE performance can be obtained when the number of all antennas for RAUs is fixed. It is also shown that the multicell DM-MIMO system can benefits from the macro diversity gain.

V. CONCLUSION

In this paper, we have investigated the achievable DL rate of multicell DM-MIMO systems with PC in Rician fading channels under imperfect CSI. Closed-form expressions of the lower bound on the achievable DL rate were obtained for the MRT and LOS component-based EGT precoding schemes. The tightness of the obtained rate expressions were rigorously confirmed by numerical results. Properties of the DL rate are established and discussed in detail for different power scaling laws for the MRT and LOS component-based EGT precoding schemes. In particular, it was shown that all of the power scaling laws which converge to constant values are related to the Rician K-factor, when the user transmit power is scaled down by a factor of $1/N$ for DM-MIMO systems. We also found that with both very large N and Rician K-factor, the DL rate can grows infinite, which implies that the effects of PC vanish for both of aforementioned precoding

schemes. Simulation results also showed that, when the number of RAUs antennas and the Rician K-factor are large, the LOS component-based EGT processing performs better than the MRT processing. Our results reveal that the LOS component-based EGT scheme is very suitable for multicell DM-MIMO systems over Rician fading channels in environment having a strong LOS scenario. Numerical results further showed that, the better SE performance gain can be achieved with more RAUs when the number of all antennas for RAUs is fixed.

APPENDIX A
USEFUL RESULTS

Lemma 1: Considering the vectors $\mathbf{x} \sim \mathcal{CN}(\overline{\mathbf{x}}, \mathbf{R}_x)$ with mean vector $\overline{\mathbf{x}} \in \mathbb{C}^N$ and covariance matrix $\mathbf{R}_x \in \mathbb{C}^{N\times N}$, and $\mathbf{y} \sim \mathcal{CN}(\overline{\mathbf{y}}, \mathbf{R}_y)$ with mean vector $\overline{\mathbf{y}} \in \mathbb{C}^N$ and covariance matrix $\mathbf{R}_y \in \mathbb{C}^{N\times N}$. When $\mathbf{x}$ and $\mathbf{y}$ are independent vectors, it holds that [30]

$$\mathbb{E}\left\{\left|\mathbf{x}^H\mathbf{y}\right|^2\right\} = \mathrm{tr}\left(\mathbf{R}_y\mathbf{R}_x\right) + \overline{\mathbf{x}}^H\mathbf{R}_y\overline{\mathbf{x}} + \overline{\mathbf{y}}^H\mathbf{R}_x\overline{\mathbf{y}} + \left|\overline{\mathbf{x}}^H\overline{\mathbf{y}}\right|^2 \tag{27}$$

Lemma 2: Considering the vectors $\mathbf{x} \sim \mathcal{CN}(\overline{\mathbf{x}}, \mathbf{R}_x)$ with mean vector $\overline{\mathbf{x}} \in \mathbb{C}^N$ and covariance matrix $\mathbf{R}_x \in \mathbb{C}^{N\times N}$, and $\mathbf{y} \sim \mathcal{CN}(\overline{\mathbf{y}}, \mathbf{R}_y)$ with mean vector $\overline{\mathbf{y}} \in \mathbb{C}^N$ and covariance matrix $\mathbf{R}_y \in \mathbb{C}^{N\times N}$. When $\mathbf{x}$ and $\mathbf{y}$ are correlated vectors, it holds that [30]

$$\begin{aligned}\mathbb{E}\left\{\left|\mathbf{x}^H\mathbf{y}\right|^2\right\} &= \left|\mathrm{tr}\left[\left(\mathbf{R}_x^H\right)^{1/2}\mathbf{R}_y^{1/2}\right]\right|^2 + \mathrm{tr}\left(\mathbf{R}_y\mathbf{R}_x\right) \\ &\quad + 2\,\mathrm{Re}\left\{\mathrm{tr}\left[\left(\mathbf{R}_x^H\right)^{1/2}\mathbf{R}_y^{1/2}\right]\overline{\mathbf{y}}^H\overline{\mathbf{x}}\right\} \\ &\quad + \overline{\mathbf{x}}^H\mathbf{R}_y\overline{\mathbf{x}} + \overline{\mathbf{y}}^H\mathbf{R}_x\overline{\mathbf{y}} + \left|\overline{\mathbf{x}}^H\overline{\mathbf{y}}\right|^2\end{aligned} \tag{28}$$

APPENDIX B
PROOF OF THEOREM 1

We derive the closed-form expression of the lower bound rate for MRT processing over Rician fading by calculating the following three terms of expression (11),

$$A = \left|\mathbb{E}\left\{\alpha_i\mathbf{g}_{iik}^H\hat{\mathbf{g}}_{iik}\right\}\right|^2 \tag{29}$$

$$\begin{aligned}B &= \mathbb{V}\mathrm{ar}\left\{\alpha_i\mathbf{g}_{iik}^H\hat{\mathbf{g}}_{iik}\right\} = \alpha_i^2\left\{\mathbb{E}\left\{\hat{\mathbf{g}}_{iik}^H\hat{\mathbf{g}}_{iik}\hat{\mathbf{g}}_{iik}^H\hat{\mathbf{g}}_{iik}\right\}\right. \\ &\quad \left. + \mathbb{E}\left\{\tilde{\mathbf{g}}_{iik}^H\hat{\mathbf{g}}_{iik}\hat{\mathbf{g}}_{iik}^H\tilde{\mathbf{g}}_{iik}\right\} - \left|\mathbb{E}\left\{\hat{\mathbf{g}}_{iik}^H\hat{\mathbf{g}}_{iik}\right\}\right|^2\right\}\end{aligned} \tag{30}$$

$$C = \sum_{(l,j)\neq(i,k)}\mathbb{E}\left\{\left|\alpha_l\mathbf{g}_{lik}^H\hat{\mathbf{g}}_{llj}\right|^2\right\}$$

$$\begin{aligned}&= \sum_{l=1}^{L}\sum_{j=1,j\neq k}^{K}\alpha_l^2\{\underbrace{\mathbb{E}\left\{\hat{\mathbf{g}}_{lik}^H\hat{\mathbf{g}}_{llj}\hat{\mathbf{g}}_{llj}^H\hat{\mathbf{g}}_{lik}\right\}}_{a} + \underbrace{\mathbb{E}\left\{\tilde{\mathbf{g}}_{lik}^H\hat{\mathbf{g}}_{llj}\hat{\mathbf{g}}_{llj}^H\tilde{\mathbf{g}}_{lik}\right\}}_{b}\} \\ &\quad + \sum_{l=1,l\neq i}^{L}\alpha_l^2\{\underbrace{\mathbb{E}\left\{\hat{\mathbf{g}}_{lik}^H\hat{\mathbf{g}}_{llk}\hat{\mathbf{g}}_{llk}^H\hat{\mathbf{g}}_{lik}\right\}}_{c} + \underbrace{\mathbb{E}\left\{\tilde{\mathbf{g}}_{lik}^H\hat{\mathbf{g}}_{llk}\hat{\mathbf{g}}_{llk}^H\tilde{\mathbf{g}}_{lik}\right\}}_{d}\}\end{aligned} \tag{31}$$

The desired signal power in (11) can be calculated by

$$\begin{aligned}A &= \left|\mathbb{E}\left\{\alpha_i\mathbf{g}_{iik}^H\hat{\mathbf{g}}_{iik}\right\}\right|^2 = \left|\mathbb{E}\left\{\alpha_i\hat{\mathbf{g}}_{iik}^H\hat{\mathbf{g}}_{iik}\right\}\right|^2 \\ &= \alpha_i^2N^2\left[\sum_{m=1}^{M}\left(\frac{\lambda_{imik}^2 + \beta_{imik}K_{ikm}}{K_{ikm}+1}\right)\right]^2\end{aligned} \tag{32}$$

where $A \triangleq \Delta_1$, and (32) is obtained because $\tilde{\mathbf{g}}_{iik}$ is statistically independent of $\hat{\mathbf{g}}_{iik}$.

We can rewrite (11) as (33), as shown at the bottom of the page. so we need to calculate the a, b, c, d four terms in (33) and analyze them under two cases: *Case 1:* $l = i$; *Case 2:* $l \neq i$.

For the term a, when $l = i$, $\hat{\mathbf{g}}_{iij}$ and $\hat{\mathbf{g}}_{iik}$ are independent, we have

$$\underset{l=i}{a} = \mathbb{E}\left\{\hat{\mathbf{g}}_{iik}^H\hat{\mathbf{g}}_{iij}\hat{\mathbf{g}}_{iij}^H\hat{\mathbf{g}}_{iik}\right\} = \mathbb{E}\left\{\left|\hat{\mathbf{g}}_{iij}^H\hat{\mathbf{g}}_{iik}\right|^2\right\} \tag{34}$$

we let $\mathbf{x} = \hat{\mathbf{g}}_{iij}$, $\mathbf{y} = \hat{\mathbf{g}}_{iik}$ and compute

$$\mathrm{tr}\left(\mathbf{R}_y\mathbf{R}_x\right) = N\sum_{m=1}^{M}\left(\frac{\lambda_{imik}^2\lambda_{imij}^2}{\left(K_{ikm}+1\right)\left(K_{ijm}+1\right)}\right) \tag{35}$$

$$\overline{\mathbf{x}}^H\mathbf{R}_y\overline{\mathbf{x}} = N\sum_{m=1}^{M}\frac{\lambda_{imik}^2\beta_{imij}K_{ijm}}{\left(K_{ikm}+1\right)\left(K_{ijm}+1\right)} \tag{36}$$

$$\overline{\mathbf{y}}^H\mathbf{R}_x\overline{\mathbf{y}} = N\sum_{m=1}^{M}\frac{\lambda_{imij}^2\beta_{imik}K_{ikm}}{\left(K_{ikm}+1\right)\left(K_{ijm}+1\right)} \tag{37}$$

$$\left|\overline{\mathbf{x}}^H\overline{\mathbf{y}}\right|^2 = \left[\sum_{m=1}^{M}\Delta_{ikjm}\sqrt{\frac{\beta_{imik}\beta_{imij}K_{ikm}K_{ijm}}{\left(K_{ikm}+1\right)\left(K_{ijm}+1\right)}}\right]^2 \tag{38}$$

Substituting (35) to (38) into (27), the term (34) can be calculated as (39), as shown at the bottom of the next page.

When $l \neq i$, $\hat{\mathbf{g}}_{llj}$ and $\hat{\mathbf{g}}_{lik}$ are independent, we have

$$\underset{l\neq i}{a} = \mathbb{E}\left\{\hat{\mathbf{g}}_{lik}^H\hat{\mathbf{g}}_{llj}\hat{\mathbf{g}}_{llj}^H\hat{\mathbf{g}}_{lik}\right\} = \mathbb{E}\left\{\left|\hat{\mathbf{g}}_{llj}^H\hat{\mathbf{g}}_{lik}\right|^2\right\} \tag{40}$$

we let $\mathbf{x} = \hat{\mathbf{g}}_{llj}$, $\mathbf{y} = \hat{\mathbf{g}}_{lik}$ and compute

$$\mathrm{tr}\left(\mathbf{R}_y\mathbf{R}_x\right) = N\sum_{m=1}^{M}\frac{\lambda_{lmlj}^2\lambda_{lmik}^2}{\left(K_{ljm}+1\right)} \tag{41}$$

$$R_{ik} = \log_2\left(1 + \frac{\Delta_1}{\sum_{l=1}^{L}\sum_{j=1,j\neq k}^{K}\alpha_l^2(a+b) + \sum_{l=1}^{L}\alpha_l^2(c+d) - \Delta_1 + \frac{1}{p_d}}\right) \tag{33}$$

$$\bar{\mathbf{x}}^H \mathbf{R}_y \bar{\mathbf{x}} = N \sum_{m=1}^{M} \frac{\lambda_{lmik}^2 \beta_{lmlj} K_{ljm}}{(K_{ljm}+1)} \tag{42}$$

$$\bar{\mathbf{y}}^H \mathbf{R}_x \bar{\mathbf{y}} = \left|\bar{\mathbf{x}}^H \bar{\mathbf{y}}\right|^2 = 0 \tag{43}$$

Substituting (41) to (43) into (27), the term (40) can be calculated as

$$\underset{l\neq i}{a} = N \sum_{m=1}^{M} \frac{\lambda_{lmik}^2 \left(\lambda_{lmlj}^2 + \beta_{lmlj} K_{ljm}\right)}{(K_{ljm}+1)} \tag{44}$$

For the term b, we use the same approach as computing the term a. when $l = i$, we have

$$\begin{aligned}\underset{l=i}{b} &= \mathbb{E}\left\{\tilde{\mathbf{g}}_{iik}^H \hat{\mathbf{g}}_{iij} \hat{\mathbf{g}}_{iij}^H \tilde{\mathbf{g}}_{iik}\right\} = \mathbb{E}\left\{\left|\hat{\mathbf{g}}_{iij}^H \tilde{\mathbf{g}}_{iik}\right|^2\right\} \\ &= N \sum_{m=1}^{M} \frac{\left(\beta_{imik} - \lambda_{imik}^2\right)\left(\lambda_{imij}^2 + \beta_{imij} K_{ijm}\right)}{(K_{ijm}+1)(K_{ikm}+1)}\end{aligned} \tag{45}$$

When $l \neq i$, we have

$$\begin{aligned}\underset{l\neq i}{b} &= \mathbb{E}\left\{\tilde{\mathbf{g}}_{lik}^H \hat{\mathbf{g}}_{llj} \hat{\mathbf{g}}_{llj}^H \tilde{\mathbf{g}}_{lik}\right\} = \mathbb{E}\left\{\left|\hat{\mathbf{g}}_{llj}^H \tilde{\mathbf{g}}_{lik}\right|^2\right\} \\ &= N \sum_{m=1}^{M} \frac{\left(\beta_{lmik} - \lambda_{lmik}^2\right)\left(\lambda_{lmlj}^2 + \beta_{lmlj} K_{ljm}\right)}{(K_{ljm}+1)}\end{aligned} \tag{46}$$

For the term c, when $l = i$, we obtain

$$\underset{l=i}{c} = \mathbb{E}\left\{\hat{\mathbf{g}}_{iik}^H \hat{\mathbf{g}}_{iik} \hat{\mathbf{g}}_{iik}^H \hat{\mathbf{g}}_{iik}\right\} = \mathbb{E}\left\{\left|\hat{\mathbf{g}}_{iik}^H \hat{\mathbf{g}}_{iik}\right|^2\right\} \tag{47}$$

we let $\mathbf{x} = \mathbf{y} = \hat{\mathbf{g}}_{iik}$, and

$$\bar{\mathbf{x}} = \bar{\mathbf{y}} = \left[\frac{\Omega_{ik}}{\Omega_{ik}+1}\right]^{1/2} \otimes \mathbf{I}_N \bar{\mathbf{g}}_{iik} \tag{48}$$

$$\mathbf{R}_x = \mathbf{R}_y = \left(\frac{1}{\Omega_{ik}+1}\right) \otimes \mathbf{I}_N \mathbf{D}_{iik}^2 \mathbf{Q}_{ik}^{-1} \tag{49}$$

Substituting (48) and (49) into (28), the term (47) can be calculated as

$$\begin{aligned}\underset{l=i}{c} &= \left[N \sum_{m=1}^{M} \left(\frac{\lambda_{imik}^2}{K_{ikm}+1}\right)\right]^2 + N \sum_{m=1}^{M} \left(\frac{\lambda_{imik}^2}{K_{ikm}+1}\right)^2 \\ &+ \left[N \sum_{m=1}^{M} \left(\frac{\beta_{imik} K_{ikm}}{K_{ikm}+1}\right)\right]^2 + 2N \sum_{m=1}^{M} \frac{\lambda_{imik}^2 \beta_{imik} K_{ikm}}{(K_{ikm}+1)^2} \\ &+ 2N^2 \sum_{m_1=1}^{M} \left(\frac{\beta_{im_1ik} K_{ikm_1}}{K_{ikm_1}+1}\right) \sum_{m_2=1}^{M} \left(\frac{\lambda_{im_2ik}^2}{K_{ikm_2}+1}\right)\end{aligned} \tag{50}$$

When $l \neq i$, $\hat{\mathbf{g}}_{llk}$ and $\hat{\mathbf{g}}_{lik}$ are correlated, we have

$$\underset{l\neq i}{c} = \mathbb{E}\left\{\hat{\mathbf{g}}_{lik}^H \hat{\mathbf{g}}_{llk} \hat{\mathbf{g}}_{llk}^H \hat{\mathbf{g}}_{lik}\right\} = \mathbb{E}\left\{\left|\hat{\mathbf{g}}_{llk}^H \hat{\mathbf{g}}_{lik}\right|^2\right\} \tag{51}$$

we let $\mathbf{x} = \hat{\mathbf{g}}_{llk}$, $\mathbf{y} = \hat{\mathbf{g}}_{lik}$ and calculate

$$\left|\mathrm{tr}\left[\left(\mathbf{R}_x^H\right)^{\frac{1}{2}} \mathbf{R}_y^{\frac{1}{2}}\right]\right|^2 = \left[N \sum_{m=1}^{M} \left(\frac{1}{K_{lkm}+1}\right)^{\frac{1}{2}} \lambda_{lmlk} \lambda_{lmik}\right]^2 \tag{52}$$

$$\mathrm{tr}\left(\mathbf{R}_y \mathbf{R}_x\right) = N \sum_{m=1}^{M} \frac{\lambda_{lmik}^2 \lambda_{lmlk}^2}{(K_{lkm}+1)} \tag{53}$$

$$\bar{\mathbf{x}}^H \mathbf{R}_y \bar{\mathbf{x}} = N \sum_{m=1}^{M} \frac{\lambda_{lmik}^2 \beta_{lmlk} K_{lkm}}{(K_{lkm}+1)} \tag{54}$$

$$\begin{aligned}&2\,\mathrm{Re}\left\{\mathrm{tr}\left[\left(\mathbf{R}_x^H\right)^{\frac{1}{2}} \mathbf{R}_y^{\frac{1}{2}}\right] \bar{\mathbf{y}}^H \bar{\mathbf{x}}\right\} \\ &= \bar{\mathbf{y}}^H \mathbf{R}_x \bar{\mathbf{y}} = \left|\bar{\mathbf{x}}^H \bar{\mathbf{y}}\right|^2 = 0\end{aligned} \tag{55}$$

Substituting (52) to (55) into (28), the term (51) can be calculated as

$$\begin{aligned}\underset{l\neq i}{c} &= N \sum_{m=1}^{M} \frac{\lambda_{lmik}^2 \left(\lambda_{lmlk}^2 + \beta_{lmlk} K_{lkm}\right)}{(K_{lkm}+1)} \\ &+ \left[N \sum_{m=1}^{M} \left(\frac{1}{K_{lkm}+1}\right)^{1/2} \lambda_{lmlk} \lambda_{lmik}\right]^2\end{aligned} \tag{56}$$

For the term d, we use the same approach as computing the term a. when $l = i$, we have

$$\begin{aligned}\underset{l=i}{d} &= \mathbb{E}\left\{\tilde{\mathbf{g}}_{iik}^H \hat{\mathbf{g}}_{ii} \hat{\mathbf{g}}_{iik}^H \tilde{\mathbf{g}}_{iik}\right\} = \mathbb{E}\left\{\left|\hat{\mathbf{g}}_{iik}^H \tilde{\mathbf{g}}_{iik}\right|^2\right\} \\ &= N \sum_{m=1}^{M} \frac{\left(\beta_{imik} - \lambda_{imik}^2\right)\left(\lambda_{imik}^2 + \beta_{imik} K_{ikm}\right)}{(K_{ikm}+1)^2}\end{aligned} \tag{57}$$

When $l \neq i$, we have

$$\begin{aligned}\underset{l\neq i}{d} &= \mathbb{E}\left\{\tilde{\mathbf{g}}_{lik}^H \hat{\mathbf{g}}_{llk} \hat{\mathbf{g}}_{llk}^H \tilde{\mathbf{g}}_{lik}\right\} = \mathbb{E}\left\{\left|\hat{\mathbf{g}}_{llk}^H \tilde{\mathbf{g}}_{lik}\right|^2\right\} \\ &= N \sum_{m=1}^{M} \frac{\left(\beta_{lmik} - \lambda_{lmik}^2\right)\left(\lambda_{lmlk}^2 + \beta_{lmlk} K_{lkm}\right)}{(K_{lkm}+1)}\end{aligned} \tag{58}$$

Substituting (39), (44)-(46), (50), (56)-(58) into (33), we finally obtain (12).

APPENDIX C
PROOF OF THEOREM 2

For LOS-EGT precoding over Rician fading, we let

$$\bar{\mathbf{g}}'_{iik} = \mathbf{D}_{iik}^{1/2} \left[\frac{\Omega_{ik}}{\Omega_{ik}+1}\right]^{1/2} \otimes \mathbf{I}_N \bar{\mathbf{h}}_{iik} \tag{59}$$

$$\mathbf{g}'_{w,iik} = \mathbf{D}_{iik}^{1/2} \left[\frac{1}{\Omega_{ik}+1}\right]^{1/2} \otimes \mathbf{I}_N \mathbf{h}_{w,iik} \tag{60}$$

$$\underset{l=i}{a} = N \sum_{m=1}^{M} \left(\frac{\lambda_{imik}^2 \lambda_{imij}^2 + \lambda_{imij}^2 \beta_{imik} K_{ikm} + \lambda_{imik}^2 \beta_{imij} K_{ijm}}{(K_{ikm}+1)(K_{ijm}+1)}\right) + \left[\sum_{m=1}^{M} \Delta_{ikjm} \sqrt{\frac{\beta_{imik} \beta_{imij} K_{ikm} K_{ijm}}{(K_{ikm}+1)(K_{ijm}+1)}}\right]^2 \tag{39}$$

We derive the closed-form expression of the lower bound rate by calculating the (29)-(31) three terms as

$$A = p_d \left| \mathbb{E}\left\{ \alpha_i \mathbf{g}_{iik}^H \mathbf{a}_{ik} \right\} \right|^2 = \frac{p_d N}{MK} \left[\sum_{m=1}^{M} \left(\frac{\beta_{imik} K_{ikm}}{K_{ikm}+1} \right)^{\frac{1}{2}} \right]^2 \tag{61}$$

$$\begin{aligned} B &= p_d \mathbb{E}\left\{ \left| \alpha_i \mathbf{g}_{iik}^H \bar{\mathbf{h}}_{iik} - \mathbb{E}\left\{ \alpha_i \mathbf{g}_{iik}^H \bar{\mathbf{h}}_{iik} \right\} \right|^2 \right\} \\ &= p_d \mathbb{E}\left\{ \left| \alpha_i \mathbf{g}_{w,iik}^{\prime H} \bar{\mathbf{h}}_{iik} \right|^2 \right\} = \frac{p_d}{MK} \sum_{m=1}^{M} \left(\frac{\beta_{imik}}{K_{ikm}+1} \right) \end{aligned} \tag{62}$$

$$C = C_1 + C_2 \tag{63}$$

$$\begin{aligned} C_1 &= p_d \mathbb{E}\left\{ \sum_{j=1, j\neq k}^{K} \left| \alpha_i \mathbf{g}_{iik}^H \mathbf{a}_{ij} \right|^2 \right\} \\ &= \frac{p_d (K-1)}{MK} \sum_{m=1}^{M} \left(\frac{\beta_{imik}}{K_{ikm}+1} \right) \\ &\quad + \frac{p_d}{MNK} \sum_{j=1, j\neq k}^{K} \sum_{m=1}^{M} \left(\Delta_{ikjm}^2 \frac{\beta_{imik} K_{ikm}}{K_{ikm}+1} \right) \end{aligned} \tag{64}$$

$$C_2 = p_d \mathbb{E}\left\{ \sum_{l=1, l\neq i}^{L} \sum_{j=1}^{K} \left| \alpha_l \mathbf{g}_{lik}^H \mathbf{a}_{lj} \right|^2 \right\} = \frac{p_d}{M} \sum_{l=1, l\neq i}^{L} \sum_{m=1}^{M} \beta_{lmik} \tag{65}$$

Substituting (61)-(65) into (11) yields (22).

REFERENCES

[1] T. L. Marzetta, "Noncooperative cellular wireless with unlimited numbers of base station antennas," *IEEE Trans. Wireless Commun.*, vol. 9, no. 11, pp. 3590–3600, Nov. 2010.

[2] H. Quoc Ngo, E. G. Larsson, and T. L. Marzetta, "Energy and spectral efficiency of very large multiuser MIMO systems," *IEEE Trans. Commun.*, vol. 61, no. 4, pp. 1436–1449, Apr. 2013.

[3] J. Hoydis, S. ten Brink, and M. Debbah, "Massive MIMO in the UL/DL of cellular networks: How many antennas do we need?" *IEEE J. Sel. Areas Commun.*, vol. 31, no. 2, pp. 160–171, Feb. 2013.

[4] D. Tsilimantos, J.-M. Gorce, K. Jaffres-Runser, and H. V. Poor, "Spectral and energy efficiency trade-offs in cellular networks," *IEEE Trans. Wireless Commun.*, vol. 15, no. 1, pp. 54–66, Jan. 2016.

[5] W. Liu, S. Han, and C. Yang, "Energy efficiency scaling law of massive MIMO systems," *IEEE Trans. Commun.*, vol. 65, no. 1, pp. 107–121, Jan. 2017.

[6] S. Zhang, Q. Wu, S. Xu, and G. Y. Li, "Fundamental green tradeoffs: Progresses, challenges, and impacts on 5G networks," *IEEE Commun. Surveys Tuts.*, vol. 19, no. 1, pp. 33–56, 1st Quart., 2017.

[7] E. Björnson, J. Hoydis, and L. Sanguinetti, "Massive MIMO has unlimited capacity," *IEEE Trans. Wireless Commun.*, vol. 17, no. 1, pp. 574–590, Jan. 2018.

[8] K. N. R. S. V. Prasad, E. Hossain, and V. K. Bhargava, "Energy efficiency in massive MIMO-based 5G networks: Opportunities and challenges," *IEEE Wireless Commun.*, vol. 24, no. 3, pp. 86–94, Jun. 2017.

[9] A. Khansefid and H. Minn, "Achievable downlink rates of MRC and ZF precoders in massive MIMO with uplink and downlink pilot contamination," *IEEE Trans. Commun.*, vol. 63, no. 12, pp. 4849–4864, Dec. 2015.

[10] D. J. Love and R. W. Heath, "Equal gain transmission in multiple-input multiple-output wireless systems," *IEEE Trans. Commun.*, vol. 51, no. 7, pp. 1102–1110, Jul. 2003.

[11] O. Onireti, F. Heliot, and M. A. Imran, "On the energy efficiency-spectral efficiency trade-off of distributed MIMO systems," *IEEE Trans. Commun.*, vol. 61, no. 9, pp. 3741–3753, Sep. 2013.

[12] J. Joung, Y. K. Chia, and S. Sun, "Energy-efficient, large-scale distributed-antenna system (L-DAS) for multiple users," *IEEE J. Sel. Topics Signal Process.*, vol. 8, no. 5, pp. 954–965, Oct. 2014.

[13] Y. Lin and W. Yu, "Downlink spectral efficiency of distributed antenna systems under a stochastic model," *IEEE Trans. Wireless Commun.*, vol. 13, no. 12, pp. 6891–6902, Dec. 2014.

[14] Q. Sun, Y. Zhang, S. Jin, J. Wang, X. Gao, and K.-K. Wong, "Downlink massive distributed antenna systems scheduling," *IET Commun.*, vol. 9, no. 7, pp. 1006–1016, May 2015.

[15] D. Wang, J. Wang, X. You, Y. Wang, M. Chen, and X. Hou, "Spectral efficiency of distributed MIMO systems," *IEEE J. Sel. Areas Commun.*, vol. 31, no. 10, pp. 2112–2127, Oct. 2013.

[16] L. Dai, "An uplink capacity analysis of the distributed antenna system (DAS): From cellular DAS to DAS with virtual cells," *IEEE Trans. Wireless Commun.*, vol. 13, no. 5, pp. 2717–2731, May 2014.

[17] M. Matthaiou, C. Zhong, M. R. McKay, and T. Ratnarajah, "Sum rate analysis of ZF receivers in distributed MIMO systems," *IEEE J. Sel. Areas Commun.*, vol. 31, no. 2, pp. 180–191, Feb. 2013.

[18] T. Alade, H. Zhu, and J. Wang, "Uplink spectral efficiency analysis of in-building distributed antenna systems," *IEEE Trans. Wireless Commun.*, vol. 14, no. 7, pp. 4063–4074, Jul. 2015.

[19] A. Yang, Y. Jing, C. Xing, Z. Fei, and J. Kuang, "Performance analysis and location optimization for massive MIMO systems with circularly distributed antennas," *IEEE Trans. Wireless Commun.*, vol. 14, no. 10, pp. 5659–5671, Oct. 2015.

[20] G. N. Kamga, M. Xia, and S. Aissa, "Spectral-efficiency analysis of massive MIMO systems in centralized and distributed schemes," *IEEE Trans. Commun.*, vol. 64, no. 5, pp. 1930–1941, May 2016.

[21] J. Zuo, J. Zhang, C. Yuen, W. Jiang, and W. Luo, "Energy-efficient downlink transmission for multicell massive DAS with pilot contamination," *IEEE Trans. Veh. Technol.*, vol. 66, no. 2, pp. 1209–1221, Feb. 2017.

[22] J. Li, D. Wang, P. Zhu, and X. You, "Benefits of beamforming training scheme in distributed large-scale MIMO systems," *IEEE Access*, vol. 6, pp. 7432–7444, 2018.

[23] J. Li, D. Wang, P. Zhu, J. Wang, and X. You, "Downlink spectral efficiency of distributed massive MIMO systems with linear beamforming under pilot contamination," *IEEE Trans. Veh. Technol.*, vol. 67, no. 2, pp. 1130–1145, Feb. 2018.

[24] G. Dong, H. Zhang, S. Jin, and D. Yuan, "Energy-Efficiency-Oriented joint user association and power allocation in distributed massive MIMO systems," *IEEE Trans. Veh. Technol.*, vol. 68, no. 6, pp. 5794–5808, Jun. 2019.

[25] Q. Zhang, S. Jin, Y. Huang, and H. Zhu, "Uplink rate analysis of multicell massive MIMO systems in ricean fading," in *Proc. IEEE Global Commun. Conf.*, Austin, TX, USA, Dec. 2014, pp. 3279–3284.

[26] Q. Zhang, S. Jin, K.-K. Wong, H. Zhu, and M. Matthaiou, "Power scaling of uplink massive MIMO systems with arbitrary-rank channel means," *IEEE J. Sel. Topics Signal Process.*, vol. 8, no. 5, pp. 966–981, Oct. 2014.

[27] X. Sun, K. Xu, W. Ma, Y. Xu, X. Xia, and D. Zhang, "Multi-pair two-way massive MIMO AF full-duplex relaying with imperfect CSI over ricean fading channels," *IEEE Access*, vol. 4, pp. 4933–4945, 2016.

[28] J. Zhang, L. Dai, Z. He, S. Jin, and X. Li, "Performance analysis of mixed-ADC massive MIMO systems over rician fading channels," *IEEE J. Sel. Areas Commun.*, vol. 35, no. 6, pp. 1327–1338, Jun. 2017.

[29] S.-N. Jin, D.-W. Yue, and H. H. Nguyen, "Multicell massive MIMO: Downlink rate analysis with linear processing under ricean fading," *IEEE Trans. Veh. Technol.*, vol. 68, no. 4, pp. 3777–3791, Apr. 2019.

[30] Ö. Özdogan, E. Björnson, and E. G. Larsson, "Massive MIMO with spatially correlated rician fading channels," *IEEE Trans. Commun.*, vol. 67, no. 5, pp. 3234–3250, May 2019.

[31] D.-W. Yue, Y. Zhang, and Y. Jia, "Beamforming based on specular component for massive MIMO systems in ricean fading," *IEEE Wireless Commun. Lett.*, vol. 4, no. 2, pp. 197–200, Apr. 2015.

[32] D.-W. Yue, "Specular component-based beamforming for broadband massive MIMO systems with doubly-ended correlation," *Electron. Lett.*, vol. 52, no. 12, pp. 1082–1084, Jun. 2016.

[33] S.-N. Jin, D.-W. Yue, and H. H. Nguyen, "Equal-gain transmission in massive MIMO systems under ricean fading," *IEEE Trans. Veh. Technol.*, vol. 67, no. 10, pp. 9656–9668, Oct. 2018.

[34] N. Ravindran, N. Jindal, and H. C. Huang, "Beamforming with finite rate feedback for LOS MIMO downlink channels," in *Proc. IEEE Global Telecommun. Conf. (GLOBECOM)*, Washington, DC, USA, Nov. 2007, pp. 4200–4204.

[35] S. M. Kay, *Fundamentals of Statistical Signal Processing, Estimation Theory* vol. 1. Upper Saddle River, NJ, USA: Pearson, 1993.
[36] D.-W. Yue and Q. Yan, "LOS component-based beamforming for downlink wireless backhauling with massive MIMO," in *Proc. 6th Int. Conf. Instrum. Meas., Comput., Commun. Control (IMCCC)*, Harbin, China, Jul. 2016, pp. 869–873.
[37] J. Jose, A. Ashikhmin, T. L. Marzetta, and S. Vishwanath, "Pilot contamination and precoding in multi-cell TDD systems," *IEEE Trans. Wireless Commun.*, vol. 10, no. 8, pp. 2640–2651, Aug. 2011.
[38] A. Kuhestani, P. L. Yeoh, and A. Mohammadi, "Optimal power allocation and secrecy sum rate in two-way untrusted relaying," in *Proc. IEEE Global Commun. Conf. (GLOBECOM)*, Singapore, Dec. 2017, pp. 1–6.
[39] H. Saedi, A. Mohammadi, and A. Kuhestani, "Characterization of untrusted relaying networks in the presence of an adversary jammer," *Wireless Netw.*, vol. 26, no. 3, pp. 2113–2124, Apr. 2020.
[40] H. Akhlaghpasand, E. Bjornson, and S. M. Razavizadeh, "Jamming suppression in massive MIMO systems," *IEEE Trans. Circuits Syst. II, Exp. Briefs*, vol. 67, no. 1, pp. 182–186, Jan. 2020.

MENG WANG received the B.S. degree in electronic information engineering from Dalian Maritime University, Dalian, China, in 2010, and the M.S. degree in electronics and computer engineering from Hanyang University, Seoul, South Korea, in 2014. He is currently pursuing the Ph.D. degree in information and communication engineering with Dalian Maritime University. He is also a Lecturer with the Department of Communication Engineering, School of Intelligent and Electronic Engineering, Dalian Neusoft University of Information, Dalian. His research interests include massive MIMO systems, wireless relaying systems, and millimeter-wave MIMO communications.

DIAN-WU YUE (Senior Member, IEEE) received the B.S. and M.S. degrees in mathematics from Nankai University, Tianjin, China, in 1986 and 1989, respectively, and the Ph.D. degree in communications and information engineering from the Beijing University of Posts and Telecommunications, Beijing, China, in 1996. From 1989 to 1993, he was a Research Assistant of applied mathematics with the Dalian University of Technology, Dalian, Liaoning, China. From 1996 to 2003, he was an Associate Professor of communications and information engineering with the Nanjing University of Posts and Telecommunications, Nanjing, Jiangsu, China. From 2000 to 2001, he was a Visiting Scholar with the University of Manitoba, Winnipeg, MB, Canada. From 2001 to 2002, he was a Postdoctoral Fellow with the University of Waterloo, Waterloo, ON, Canada. Since December 2003, he has been a Full Professor of communications and information engineering with Dalian Maritime University, Dalian, Liaoning. His current research interests include massive MIMO systems, millimeter-wave MIMO communications, and cooperative relaying communications.

SI-NIAN JIN received the B.S. degree in communication engineering from Shandong University, Weihai, China, in 2014, and the M.S. degree in information and communication engineering from Dalian Maritime University, Dalian, China, in 2017, where he is currently pursuing the Ph.D. degree in information and communication engineering. His research interests include massive MIMO systems and cooperative communications.